TEAPREVU: A numerical simulation model of Terminal Electron-Accepting Processes in a Representative Elementary Volume of Uranium-contaminated subsurface sediment

Developed by[1]:

Eric E. Roden[2], The University of Alabama
Yilin Fang and Tim Scheibe, Pacific Northwest National Laboratory
Scott Brooks, Oak Ridge National Laboratory

January 2005

[1] Through support of the U.S. Department of Energy, Office of Biological and Environmental Research, Natural and Accelerated Bioremediation Research Program

[2] Corresponding author; (205) 348-0556; **eroden@bsc.as.ua.edu**

Description of TEAPREVU Model

1. Overview

TEAPREVU is a reaction-based model of Terminal Electron Accepting Processes (TEAP) and other biogeochemical reactions in a hypothetical Representative Elementary Volume (REV) of Uranium-contaminated subsurface sediment. The model (which includes 30 primary dependent variables listed in Table 1) was developed to simulate the results of a batch slurry experiment with FRC Area 2 sediment (Mohanty et al., 2004), with the idea that the developed framework will eventually be incorporated into a field-scale reactive transport simulation of in situ biostimulation at Area 2. The model envisions flow of ethanol-containing fluid through a single reactor cell (the fluid flow rate is set equal to zero to model the batch slurry experiment). The incoming fluid contains soluble electron acceptors (O_2, NO_3^-, U(VI), SO_4^{2-}) whose abundance, together with the abundance of solid-phase electron acceptors (MnO_2, FeOOH, S^0) in the sediment, control the relative rates of various terminal electron accepting processes (TEAP) and other biogeochemical reactions over time in the reactor. The model accounts for complete (to HCO_3^-) or incomplete (to acetate) oxidation of ethanol, as well as oxidation of acetate to HCO_3^- and/or CH_4, via 18 different TEAP pathways (see Fig. 1 and Table 2). Each of the TEAP reactions are dependent on the biomass of one or more distinct microbial populations (8 total; see Table 1) chosen based on current knowledge of the kinds of organisms likely to proliferate in response to biostimulation of subsurface sediments. Growth of these populations is described using the bioenergetics-based approach developed by Rittman and McCarty (2001) for simulation of wastewater (i.e. sewage) treatment, in which the partitioning of organic carbon flow between energy generation and cell biomass production (see Fig. 2) is dependent on the free energy of the corresponding TEAP, which is computed dynamically during the simulation as a function of the abundance (concentration and/or activity) of the reactants and products involved in the process. This approach alleviates the need for making a priori assumptions about the biomass yield for the different physiological functional populations. Kinetic constants for uptake of electron donors, electron acceptors, and inorganic nitrogen compounds, as well for the inhibition of specific RTEAPs (37 total; see Table 3) by the presence of more favorable electron acceptors, were either chosen arbitrarily or constrained by the physiological properties of pure culture representatives and/or by values required to reproduce the results of the batch slurry experiment. Each of the RTEAPs results in production of various inorganic compounds, which either accumulate in solution or undergo reactions (sorption and/or mineral precipitation) with the solid-phase. The model also accounts for a wide variety of secondary redox reactions (sensu Van Cappellen and Wang (1996)) that may potentially occur in sedimentary environments (e.g. oxidation of reduced species such as Mn(II), Fe(II), U(IV), S(-II), S^0, and CH_4 by aqueous or solid-phase electron acceptors such as O_2, NO_3^-, MnO_2, and FeOOH; see Table 4 for a complete list of reactions), as well as for precipitation/dissolution of mineral phases that may be associated with microbial activity in sediments (see Table 5). In this way the model is capable of simulating time-dependent changes in the abundance of various oxidized and reduced species and mineral phases as a function of the input of external electron acceptors/donors and other aqueous species. This capacity is critical for field-scale simulation of biogeochemical processes in subsurface environments (Hunter et al., 1998).

The current version of the model consists of a system of differential (kinetic reactions) and algebraic (equilibrium speciation reactions) equations (summarized in Tables 3-12) that were assembled manually and directly based on our current conception of the reaction network. The differential equations are solved using a fifth-order Runge-Kutta algorithm (Press et al., 1992) as previously described (Roden, 2004), and the equilibrium speciation equations are solved with the MICROQL algorithm (Westall, 1986), which operated within the ODE solver routine. This manual system is being converted to the reaction-based batch biogeochemical simulator BIOGEOCHEM (Fang et al., 2003) en route to inclusion of the developed reaction network in field-scale modeling of subsurface biostimulation at Area 2.

2. Rational for TEAPs and microbial physiological functional groups

As outlined in Table 2, the model includes 18 separate TEAP reactions, each of which is catalyzed by at least one physiological functional group of microorganisms. This approach is analogous to that employed by Lensing et al. (1994) for simulation of TEAPs in leachate-contaminated aquifer sediments in Germany, which itself was based on the pioneering work of F. Molz, M. Celia, and colleagues on modeling of O_2 and NO_3^- respiration in porous media (Molz et al., 1986; Widdowson et al., 1988; Celia et al., 1989; Kindred and Celia, 1989). The TEAPs represent the standard suite of inorganic electron-accepting pathways known to be active in natural systems (Lovley and Chapelle (1995)) coupled to the metabolism of ethanol or acetate. The physiological functional groups were defined based on the known physiology of soil/sediment microorganisms. Strictly aerobic microorganisms (AMs) were assumed to utilize only O_2 as an electron acceptor, whereas denitrifying microorganisms (DMs) were assumed to be able to utilize either O_2 or NO_3^-, in keeping with the almost universal facultative anaerobic physiology of such organisms (Tiedje, 1988). These organisms were assumed to oxidize both ethanol and acetate directly to HCO_3^-. Three different groups of "dissimilatory reducing microorganisms" (DRM1, DRM2, DRM3) were included: the first group was assumed to catalyze only dissimilatory reduction of nitrate to ammonium (DNRA) coupled to partial oxidation of ethanol to acetate, and as such are assumed to represent obligate anaerobes that catalyze DNRA during fermentative rather than oxidative metabolism (Tiedje, 1988). The second group was assumed to catalyze both DNRA and dissimilatory reduction of Mn(IV)/Fe(III) oxides and U(VI) coupled to either partial oxidation of ethanol to acetate or complete oxidation of acetate to HCO_3^-. These organisms are assumed to represent mesophilic dissimilatory metal-reducing microorganisms such as *Geobacter* which are well-known for their ability to oxidize organic carbon compounds with Mn(IV)/Fe(III) or NO_3^- as an electron acceptor (Lovley, 2002). The third group of DRMs was assumed to be able to carry-out SO_4^{2-} and S^0 reduction in addition to NO_3^-, Mn(IV)/Fe(III), and U(VI) reduction. This group is the least well-recognized in terms of pure culture representatives, with *Desulfotomaculum reducens* (Tebo and Obraztsova, 1998) being the only isolate known to date. Although inclusion of this group of organisms was not required to simulate the results of the Area 2 slurry experiment, it was included so as to maximize flexibility in modeling the interplay between Fe(III) and SO_4^{2-} reduction in FRC sediments. The other groups of organisms included in the model are SO_4^{2-} reducing microorganisms proper (SO4RM), S^0 reducing microorganisms (S0RM), and methanogenic microorganisms (MGM), each of which were assumed to either partially oxidize ethanol to acetate, or to oxidize acetate to HCO_3^- (SO4RM and S0RM) or to a mixture of HCO_3^- and CH_4 (MGM). Note that although S^0 is not likely to be abundant in native FRC subsurface sediments (or any other native subsurface sediment), it can be generated during reaction of hydrogen sulfide (HS^-) with Mn(IV) or Fe(III) oxides (e.g. at reaction front where HS^- containing groundwater encounters Mn(IV) and/or Fe(III) oxide-bearing sediment) and subsequently serve as an electron acceptor for organic carbon oxidation. The SO_4^{2-}- and S^0-reducing organisms are assumed by default to be able to reduce U(VI), although this can be turned-off as necessary to consider the potential impact of a switch from Fe(III)-reducing to SO_4^{2-}-reducing conditions on U(VI) reduction.

The different TEAP reactions were subject to inhibition by the presence of higher redox potential electron acceptors according to standard noncompetitive inhibition functions (Rawn, 1983). Such inhibition functions account for either preferential utilization of more energetically favorable electron acceptors (which is generally under linked genetic/physiological control, as in the case of O_2 vs. NO_3^- respiration in denitrifying microorganisms (Tiedje, 1988), or NO_3^- vs. Fe(III) respiration in DRMs; D. Lovley, personal communication), for poisoning (or "short-circuiting") of respiratory electron transfer reactions (as in the case of Fe(III) inhibition of acetoclastic methanogenesis; (Bond and Lovley, 2002)), or for general interference posed by the presence of high redox potential couples. It is important to emphasize the distinction between the use of inhibition functions in this physiologically-based manner as compared to how such functions have been used in previous models of TEAP reactions in soil/sedimentary (VanCappellen and Gaillard, 1996; Hunter et al., 1998) environments. In the latter models, degradation

of organic substrates (natural organics and/or hydrocarbon contaminants) and associated consumption of electron acceptors are depicted strictly as a kinetic function of the abundance of the substrate(s) and the electron acceptor(s), with no consideration of the biomass or physiological properties of the organisms catalyzing the TEAPs. As such, inhibition functions (hyperbolic or otherwise) were used in a general way to depict the negative influence of higher redox potential electron acceptors on biodegradation coupled to utilization of lower redox potential electron acceptors – as opposed to their use here to describe effects on specific TEAPs carried out by specific groups of microorganisms.

The relative rates of different TEAP reactions were also assumed to be influenced by the presence or absence of a given organic electron donor. Specifically, ethanol was assumed to inhibit utilization of acetate according to a standard noncompetitive inhibition function. This assumption was required to reproduce the pattern of acetate accumulation during the early stages of the slurry experiment, and is consistent with the expectation that cells would preferentially utilize an energetically more favorable electron donor such as ethanol over a less energetically favorable donor such as acetate. The algorithm for computing the influence of alternative electron donors on TEAP pathways is completely general and can in principle be expanded to include the effect of the presence of multiple electron donors, e.g. the variety of end-products that might arise from fermentation of individual sugars such as glucose or polymeric mixtures of carbohydrates such as those present in molasses or corn syrup.

3. Modeling microbial biosynthesis and growth yield

The bioenergetics approach for modeling microbial biosynthesis and growth yield with either NH_4^+, NO_3^-, or N_2 as a nitrogen source (Rittmann and McCarty, 2001) was modified slightly for use in the TEAP model. First, the free energy available from each TEAP was computed dynamically during the simulation, and these values (rather than values based on standard state calculations) were used to simulate the cell growth yield, assuming a standard energy transfer efficiency of 0.6 (Rittmann and McCarty, 2001) for all TEAP reactions. Although time-dependent free energy effects were insignificant for highly favorable TEAPs such as O_2 and NO_3^- reduction, changes in the free energy of Fe(III) reduction, SO_4^{2-} reduction, and methanogenesis led to 2-5 fold decreases in the fraction of carbon flow into cell biosynthesis vs. energy generation for the batch slurry simulations. The general strategy of Rittmann and McCarty (2001) for computing the free energy requirements for biosynthesis as a function of the nitrogen source (see Table 6 for a summary of biosynthetic reactions) was retained, but the nitrogen source used for biosynthesis was not assumed to be constant during the simulation. Instead, cells were assumed to take up NH_4^+ preferentially over NO_3^-, and in turn to take up NO_3^- in preference to N_2 (i.e. to N_2 fixation). The amount of these different N sources consumed for biosynthesis of the different microbial populations was computed based on the total fixed N requirement at each time step and hyperbolic kinetic functions which account for preferential uptake the different N sources (see Table 10). A similar approach was used to simulate the influence of the presence of alternative (i.e. relative to the primary organic electron donor involved in a given TEAP) fixed carbon sources on the energetics of cellular carbon biosynthesis (see Table 8). In this case, the sequence (and relative percent) of carbon substrate utilization for biosynthesis was assumed to be identical to the sequence (and relative percent) of primary carbon substrate utilization for a given TEAP process.

4. Uranium speciation and reduction

In its current configuruation, the model includes two basic process which affect aqueous/solid-phase uranium speciation: (1) adsorption of U(VI) to Fe(III) oxide surfaces according to a non-electrostatic version of the two-site Waite et al. (1994) model; and (2) enzymatic reduction of dissolved (but not sorbed) U(VI) to insoluble UO_2(s) (uraninite) according to a standard Monod-style rate expression. Abiotic reduction of U(VI) by Fe(II), a potentially important mechanism for U(VI) reduction in Fe(III)-

reducing systems (Fredrickson et al., 2000), was omitted from the model due to uncertainties in the rate/extent of this process in natural Fe(II)-rich sediments (Jeon et al., 2005).

Stability constants for aqueous U(VI) species were those used by Waite et al. (1994), whereas the stability constants for sorption of U(VI) to oxide surfaces were obtained from fitting of data from a U(VI) sorption isotherm experiment with Oyster, VA sediment (B.H. Jeon and E.E. Roden, unpubl data). Experiments designed to parameterize U(VI) sorption to FRC Area 2 sediments are being conducted through the Scheibe et al. and Burgos et al. NABIR projects, and this information will be incorporated into the model as it becomes available. Kinetic constants for U(VI) bioreduction were constrained by published results for *Shewanella* and *Geobacter* (Truex et al., 1997; Liu et al., 2002; Roden and Scheibe, 2005).

5. Selection of parameter values

The model contains a large number of parameters (summarized in Table 13), not all of which could be independently defined or constrained by existing experimental results or information from the literature. The selection of parameter values was therefore based on a combination of existing information (referred to as "independent" parameter values), values that could constrained from literature or other sources of information (referred to as "constrained" parameter values), values that were assigned arbitrarily based on general knowledge not specific to the particular process under consideration (referred to as "arbitrary" parameter values), and finally values that were determined by trial-and-error in order to reproduce the results of the Area 2 sediment slurry experiment (referred to as "model-derived" parameter values). Although this approach may not be appealing from a rigorous scientific point of view, it is defensible in the case of complex biogeochemical models where the processes involved are more well-understood (relatively) than are the values for parameters involved those processes (VanCappellen and Wang, 1995, 1996).

6. Area 2 slurry incubation experiment simulation results

The central goal in simulating the Area 2 sediment slurry experiment was to reproduce the basic patterns of organic substrate metabolism, consumption of electron acceptors, and accumulation of reduced end-products of anaerobic respiration. In general the optimized model reproduced these patterns rather well (Fig. 3A,B). Although the timing and magnitude of the predicted accumulation of acetate resulting from partial oxidation of ethanol (and the subsequent utilization of acetate) did not exactly match the experiment results (Fig. 3A), the general agreement between the simulation and the data suggests that the developed reaction network provides a reasonable explanation for this pattern of substrate metabolism. The strategy for simulating the interaction between the different TEAPs also seems generally valid, given the close resemblance of the predicted and observed patterns of electron acceptor (NO_3^-, Fe(III), SO_4^{2-}) consumption and reduced end-product accumulation (Fe(II) and CH_4; note that the abundance of reduced sulfur compounds (e.g. HS^-, FeS) was not determined). Together these results suggest that the current version of the model is appropriate for incorporation into exploratory field-scale simulations (i.e. numerical experimentation) of ethanol metabolism and major TEAP reactions at the Area 2 field site. However, the predicted aqueous/solid speciation of uranium did not match the experimental data (Fig. 3C). A significant fraction (ca. 50%) of solid-associated U(VI) failed to desorb during biostimulation and therefore remained unreduced at the end of the incubation, a result consistent with other recent studies of enzymatic reduction of sorbed U(VI) (Jeon et al., 2004; Ortiz-Bernad et al., 2004). Understanding the controls on reduction of solid-associated U(VI) (both biotic and abiotic) and development of strategies for accurately simulating the fate of uranium in biostimulated FRC Area 2 sediments is a key goal the new Burgos et al. NABIR project ("Reaction-Based Reactive Transport Modeling of Iron Reduction and Uranium Immobilization at Area 2 of the NABIR Field Research Center").

6. References

Berg, P., S. Rysgaard, and B. Thamdrup. 2003. Dynamic modeling of early diagenesis and nutrient cycling. A case study in an arctic marine sediment. Am. J. Sci. 303:905-955.
Bond, D. R., and D. R. Lovley. 2002. Reduction of Fe(III) by methanogens in the presence and absence of extracellular quinones. Environ. Microbiol. 4:115-124.
Celia, M. A., J. S. Kindred, and I. Herrera. 1989. Contaminant transport and biodegradation 1. A numerical model for reactive transport in porous media. Wat. Resour. Res. 25:1141-1148.
Davis, J. A., and D. B. Kent. 1990. Surface complexation modeling in aqueous geochemistry. In M. F. Hochella, and A. F. White (eds.). Mineral-water interface geochemistry, pp. 177-260. Mineralogical Society of America, Washington, DC.
Fang, Y., G. T. Yeh, and W. D. Burgos. 2003. A general paradigm to model reaction-based biogeochemical processes in batch systems. Wat. Resour. Res. 39:1083-1108.
Fredrickson, J. K., J. M. Zachara, D. W. Kennedy, M. C. Duff, Y. A. Gorby, S. W. Li, and K. M. Krupka. 2000. Reduction of U(VI) in goethite (α-FeOOH) suspensions by a dissimilatory metal-reducing bacterium. Geochim. Cosmochim. Acta 64:3085-3098.
Grenthe, I., I. Puigdomenech, M. C. A. Sandino, and M. H. Rand. 1995. Appendix D. Chemical Thermodynamics of Uranium. Chemical Thermodynamics of Americium. Elsevier Science Publ., Amsterdam.
Hunter, K. S., Y. Wang, and P. VanCappellen. 1998. Kinetic modeling of microbially-driven redox chemistry of subsurface environments: coupling transport, microbial metabolism and geochemistry. J. Hydrol. 209:53-80.
Jeon, B. H., M. O. Barnett, W. D. Burgos, B. A. Dempsey, and E. E. Roden. 2005. Chemical reduction of U(VI) by Fe(II) at the solid-water interface using synthetic and natural iron(III) oxides. Environ. Sci. Technol. Submitted for publication.
Jeon, B. H., S. D. Kelly, K. M. Kemner, M. O. Barnett, W. D. Burgos, B. A. Dempsey, and E. E. Roden. 2004. Microbial reduction of U(VI) at the solid-water interface. Environ. Sci. Technol. In press.
Kindred, J. S., and M. A. Celia. 1989. Contaminant transport and biodegradation 2. Conceptual model and test simulations. Wat. Resour. Res. 25:1149-1159.
Langmuir, D. 1997. Aqueous Environmental Geochemistry. Prentice Hall, Upper Saddle River, NJ.
Lensing, H. J., M. Vogt, and B. Herrling. 1994. Modeling of biologically mediated redox processes in the subsurface. J Hydrol 159:125-143.
Liu, C., Y. A. Gorby, J. M. Zachara, J. K. Fredrickson, and C. F. Brown. 2002. Reduction kinetics of Fe(III), Co(III), U(VI), Cr(VI), Tc(VII) in cultures of dissimilatory metal reducing bacteria. Biotechnol. Bioengin. 80:637-649.
Lovley, D. R. 2002. Fe(III)- and Mn(IV)-reducing prokaryotes. In S. F. M. Dworkin, E. Rosenberg, K.H Schleifer, E. Stackebrandt (ed.). The Prokaryotes, p. In press. Springer-Verlag, New York.
Lovley, D. R., and F. H. Chapelle. 1995. Deep subsurface microbial processes. Rev. Geophys. 33:365-381.
Mohanty, S., B. Kollah, and E. E. Roden. 2004. Biogeochemical processes and microbial community structure in ethanol-stimulated subsurface sediments. Manuscript in preparation.
Molz, F. J., M. A. Widdowson, and L. D. Benefield. 1986. Simulation of microbial growth dynamics coupled to nutrient and oxygen transport in porous media. Wat. Resour. Res. 22:1207-1216.

Ortiz-Bernad, I., R. T. Anderson, H. A. Vrionis, and D. R. Lovley. 2004. Resistance of solid-phase U(VI) to microbial reduction during in situ bioremediation of uranium-contaminated groundwater. Appl. Environ. Microbiol. 70:7558-7560.
Press, W. H., S. A. Teukolsky, W. T. Vetterling, and B. P. Flannery. 1992. Numerical Recipes in FORTRAN. Cambridge University Press, Port Chester, NY.
Rawn, J. D. 1983. Biochemistry. Harper and Row, New York.
Rittmann, B. E., and P. L. McCarty. 2001. Environmental Biotechnology. McGraw-Hill, Boston.
Roden, E. E. 2004. Analysis of long-term bacterial versus chemical Fe(III) oxide reduction kinetics. GCA 68:3205-3216.
Roden, E. E., and J. H. Tuttle. 1993. Inorganic sulfur turnover in oligohaline estuarine sediments. Biogeochemistry 22:81-105.
Roden, E. E., and E. Sedo. 2003. Framework for numerical simulation of bacterial Fe(III) oxide reduction in circumneutral soil and sedimentary environments. EOS Trans. AGU 84(46), Fall Meet Suppl.:Abstract B32A-0375.
Roden, E. E., and T. D. Scheibe. 2005. Conceptual and numerical model of uranium(VI) reductive immobilization in fractured subsurface sediments. Chemosphere In press.
Stumm, W., and J. J. Morgan. 1996. Aquatic Chemistry. John Wiley & Sons, Inc., New York.
Tebo, B. M., and A. Y. Obraztsova. 1998. Sulfate-reducing bacterium grows with Cr(VI), U(VI), Mn(IV) and Fe(III) as electron acceptors. FEMS Microbiol. Lett. 162:193-198.
Thauer, R. K., K. Jungermann, and K. Decker. 1977. Energy conservation in chemotrophic anaerobic bacteria. Bacteriol. Rev. 41:100-180.
Tiedje, J. M. 1988. Ecology of denitrification and dissimilatory nitrate reduction to ammonium. In A. J. B. Zehnder (ed.). Biology of anaerobic microorganisms. John Wiley & Sons, New York.
Truex, M. J., B. M. Peyton, N. B. Valentine, and Y. A. Gorby. 1997. Kinetics of U(VI) reduction by a dissimilatory Fe(III)-reducing bacterium under non-growth conditions. Biotech. Bioengin. 55:490-496.
VanCappellen, P., and Y. Wang. 1995. Metal cycling in surface sediments: modeling the interplay of transport and reaction. In H. E. Allen (ed.). Metal contaminated aquatic sediments, pp. 21-64. Ann Arbor Press, Chelsea, MI.
VanCappellen, P., and Y. Wang. 1996. Cycling of iron and manganese in surface sediments: a general theory for the coupled transport and reaction of carbon, oxygen, nitrogen, sulfur, iron, and manganese. Am. J. Sci. 296:197-243.
VanCappellen, P., and J. F. Gaillard. 1996. Biogeochemical dynamics in aquatic sediments. In P. C. Lichtner, C. I. Steefel, and E. H. Oelkers (eds.). Reactive transport in porous media, pp. 335-376. The Mineralogical Society of America, Washington, DC.
Waite, T. D., J. A. Davis, T. E. Payne, G. A. Waychunas, and N. Xu. 1994. Uranium(VI) adsorption to ferrihydrite: Application of a surface complexation model. Geochim. Cosmochim. Acta 58:5465-5478.
Weber, K. A., E. E. Roden, and F. W. Picardal. 1998. Microbially-catalyzed nitrate-dependent oxidation of solid-phase Fe(II) compounds. Environ. Sci. Technol. Submitted for publication.
Westall, J. C. 1986. MICROQL I. A chemical equilibrium program in BASIC. Report 86-02, Department of Chemistry, Oregon State University, Corvalis, OR.
Widdowson, M. A., F. J. Molz, and L. D. Benefield. 1988. A numerical transport model of oxygen- and nitrate-based respiration linked to substrate and nutrient availability in porous media. Wat. Resour. Res. 24:1553-1565.

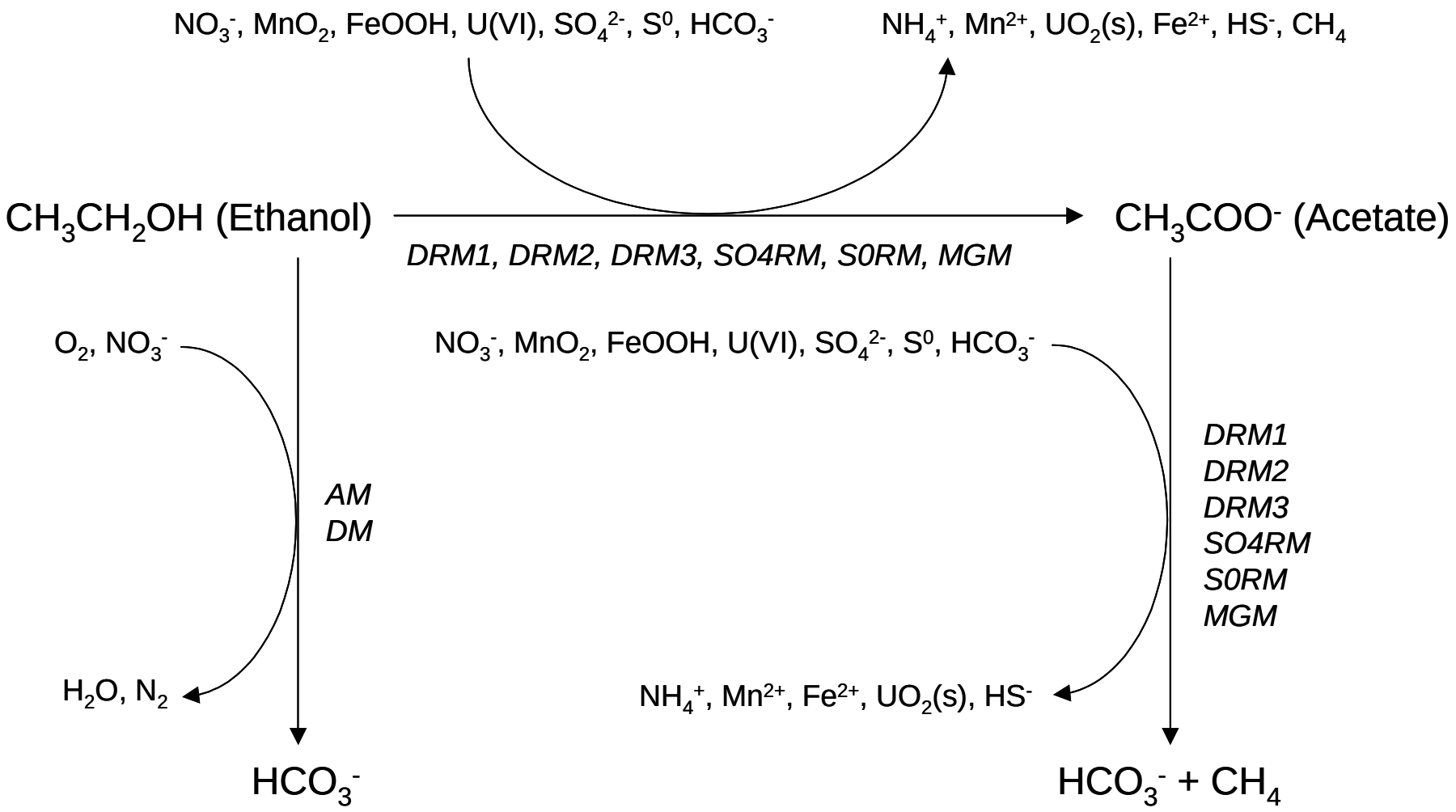

Fig. 1. Diagram of substrate metabolism and electron flow in the current implementation of the TEAPREV simulation model

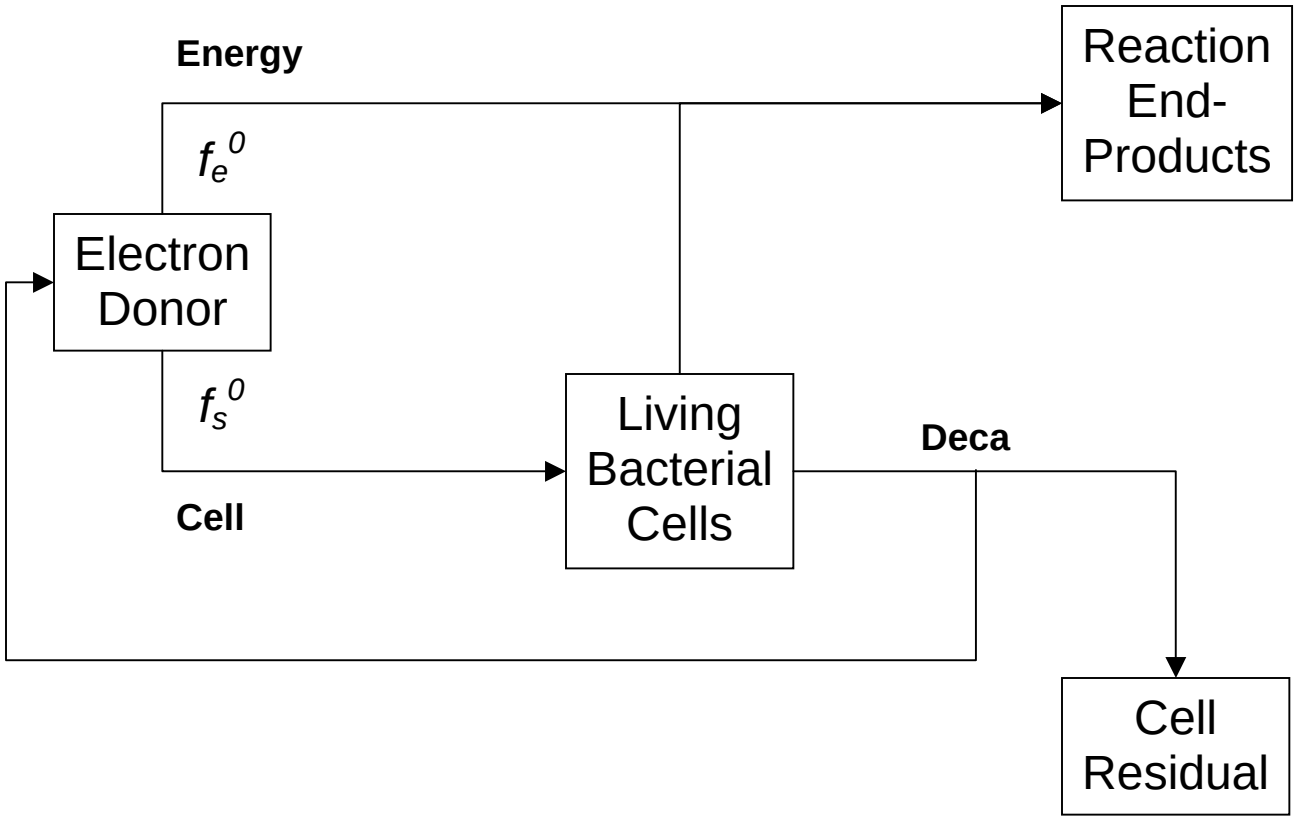

Fig. 2. Diagram of substrate partitioning between energy production and cell biosynthesis during microbial respiration. Modified from Fig. 2.1 in Rittmann and McCarty (2001).

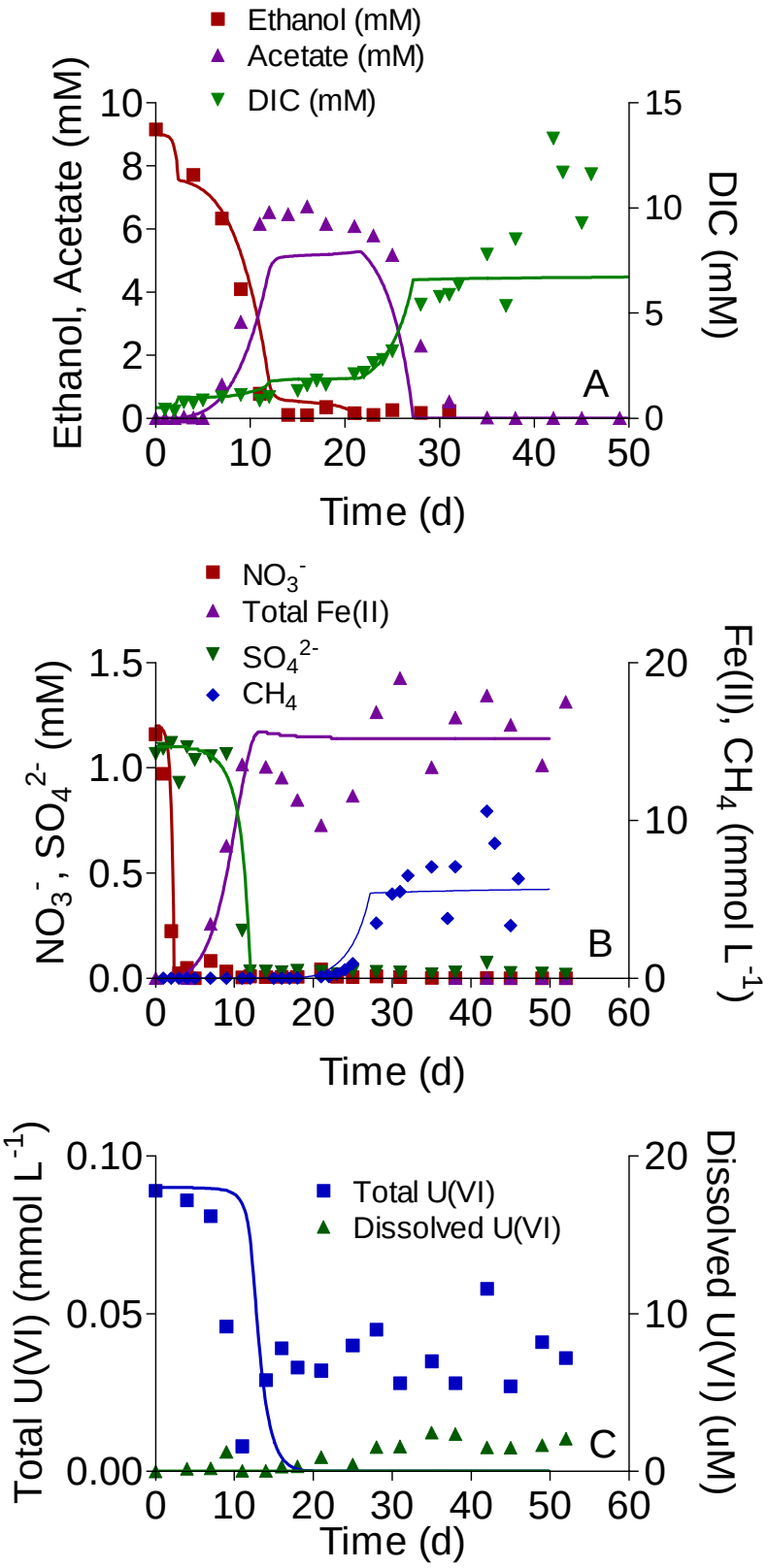

Figure 3. Results of TEAPREVU simulation of the Area 2 sediment slurry experiment. Data points show means of duplicate slurries; solid lines show simulation results.

Table 1. Primary dependent variables

Number	Type	Name	Fortran Name	Initial Value
(1)	Electron Donor	CH_3CH_2OH (Ethanol)	CH3CH2OH	0.009 (mol L^{-1})
(2)	Electron Donor	CH_3COO^- (Acetate)	CH3COO	0.0 (mol L^{-1})
(3)	Electron Acceptor	O_2	O2	0.0 (mol L^{-1})
(4)	Electron Acceptor	NO_3^-	NO3	0.0012 (mol L^{-1})
(5)	Electron Acceptor	NO_2^-	NO2	0.0 (mol L^{-1})
(6)	Electron Acceptor	MnO_2(s)	MnO2	0.0 (mol L^{-1})
(7)	Electron Acceptor	FeOOH(s)	FeOOH	0.3 (mol L^{-1})
(8)	Electron Acceptor	SO_4^{2-}	SO4	0.0011 (mol L^{-1})
(9)	Electron Acceptor	S^0(s)	S0	0.0 (mol L^{-1})
(10)	Electron Acceptor	UVI	UVI	0.00009 (mol L^{-1})
(11)	Respiration End Product	HCO_3^-	HCO3	0.005 (mol L^{-1})
(12)	Respiration End Product	N_2	N2	0.0005 (mol L^{-1})
(13)	Respiration End Product	NH_4^+	NH4	0.0001 (mol L^{-1})
(14)	Respiration End Product	Mn(II)	Mn2	0.0 (mol L^{-1})
(15)	Respiration End Product	Fe(II)	Fe2	0.0 (mol L^{-1})
(16)	Respiration End Product	HS^-	HS	0.0 (mol L^{-1})
(17)	Respiration End Product	CH_4	CH4	0.0 (mol L^{-1})
(18)	Respiration End Product	UO_2(s)	UO2	0.0 (mol L^{-1})
(19)	Reactant/Product	TOTH	TOTH	0.0212 (mol L^{-1})
(20)	Mineral Precipitate	$MnCO_3$(s)	MnCO3	0.0 (mol L^{-1})
(21)	Mineral Precipitate	$FeCO_3$(s)	FeCO3	0.0 (mol L^{-1})
(22)	Mineral Precipitate	FeS(s)	FeS	0.0 (mol L^{-1})
(23)	Microbial Biomass	Aerobic Microorganisms	AM	0.00005 (g L^{-1})
(24)	Microbial Biomass	Denitrifying Microorganisms	DM	0.00005 (g L^{-1})
(25)	Microbial Biomass	Group 1 Dissimilatory-Reducing Microorganisms	DRM1	0.000005 (g L^{-1})
(26)	Microbial Biomass	Group 2 Dissimilatory-Reducing Microorganisms	DRM2	0.0000025 (g L^{-1})
(27)	Microbial Biomass	Group 3 Dissimilatory-Reducing Microorganisms	DRM3	0.0000025 (g L^{-1})
(28)	Microbial Biomass	Sulfate-Reducing Microorganisms	SO4RM	0.000005 (g L^{-1})
(29)	Microbial Biomass	Elemental S-Reducing Microorganisms	S0RM	0.000005 (g L^{-1})
(30)	Microbial Biomass	Methanogenic Microorganisms	MGM	0.000005 (g L^{-1})

Table 2. Metabolic energy-generating terminal electron-accepting processes (TEAPs)

Number	Reaction	Catalyzed By
(1)	$CH_3CH_2OH + 3O_2 \rightarrow 2HCO_3^- + H_2O + 2H^+$	AM, DM
(2)	$CH_3CH_2OH + 2.4NO_3^- + 0.4H^+ \rightarrow 2HCO_3^- + 1.2N_2 + 2.2H_2O$	DM
(3)	$CH_3CH_2OH + 0.5NO_3^- \rightarrow CH_3COO^- + 0.5NH_4^+ + 0.5H_2O$	DRM1, DRM2, DRM3
(4)	$CH_3CH_2OH + 2MnO_2 + 3H^+ \rightarrow CH_3COO^- + 2Mn^{2+} + 3H_2O$	DRM2, DRM3
(5)	$CH_3CH_2OH + 4FeOOH + 7H^+ \rightarrow CH_3COO^- + 4Fe^{2+} + 7H_2O$	DRM2, DRM3
(6)	$CH_3CH_2OH + 0.5SO_4^{2-} \rightarrow CH_3COO^- + 0.5HS^- + 0.5H^+ + H_2O$	DRM3, SO4RM
(7)	$CH_3CH_2OH + 2S^0 + H_2O \rightarrow CH_3COO^- + 2HS^- + 3H^+$	DMR3, S0RM
(8)	$CH_3CH_2OH + 0.5HCO_3^- \rightarrow CH_3COO^- + 0.5CH_4 + 0.5H^+ + 0.5H_2O$	MGM
(9)	$CH_3COO^- + 2O_2 \rightarrow 2HCO_3^- + H^+$	AM, DM
(10)	$CH_3COO^- + 1.6NO_3^- + 0.6H^+ \rightarrow 2HCO_3^- + 0.8N_2 + 0.8H_2O$	DM
(11)	$CH_3COO^- + NO_3^- + H_2O + H^+ \rightarrow 2HCO_3^- + NH_4^+$	DRM2, DRM3
(12)	$CH_3COO^- + 4MnO_2 + 7H^+ \rightarrow 2HCO_3^- + 4Mn^{2+} + 4H_2O$	DRM2, DRM3
(13)	$CH_3COO^- + 8FeOOH + 15H^+ \rightarrow 2HCO_3^- + 8Fe^{2+} + 12H_2O$	DRM2, DRM3
(14)	$CH_3COO^- + SO_4^{2-} \rightarrow 2HCO_3^- + HS^-$	DRM3, SO4RM
(15)	$CH_3COO^- + 4S^0 + 4H_2O \rightarrow 2HCO_3^- + 4HS^- + 5H^+$	DRM3, S0RM
(16)	$CH_3COO^- + H_2O \rightarrow HCO_3^- + CH_4$	MGM
(17)	$CH_3CH_2OH + 2UO_2(CO_3)_2^{2-} + H_2O \rightarrow CH3COO^- + 4HCO_3^- + 2UO_2(s) + H^+$	DRM2, DRM3, [SO4RM, S0RM]*
(18)	$CH_3COO^- + 4UO_2(CO_3)_2^{2-} + 4H_2O \rightarrow 10HCO_3^- + 4UO_2(s) + H^+$	DRM2, DRM3, [SO4RM, S0RM]*

* Reduction of U(VI) by SO4RM and S0RM is optional

Table 3. Terminal electron-accepting process reactions (RTEAPs)

Number	Reaction	Catalyzed By
(1,1)	$CH_3CH_2OH + 3O_2 \rightarrow 2HCO_3^- + H_2O + 2H^+$	AM
(1,2)	$CH_3CH_2OH + 3O_2 \rightarrow 2HCO_3^- + H_2O + 2H^+$	DM
(2,1)	$CH_3CH_2OH + 2.4NO_3^- + 0.4H^+ \rightarrow 2HCO_3^- + 1.2N_2 + 2.2H_2O$	DM
(3,1)	$CH_3CH_2OH + 0.5\ NO_3^- \rightarrow CH_3COO^- + 0.5NH_4^+ + 0.5H_2O$	DRM1
(3,2)	$CH_3CH_2OH + 0.5\ NO_3^- \rightarrow CH_3COO^- + 0.5NH_4^+ + 0.5H_2O$	DRM2
(3,3)	$CH_3CH_2OH + 0.5\ NO_3^- \rightarrow CH_3COO^- + 0.5NH_4^+ + 0.5H_2O$	DRM3
(4,1)	$CH_3CH_2OH + 2MnO_2 + 3H^+ \rightarrow CH_3COO^- + 2Mn^{2+} + 3H_2O$	DRM2
(4,2)	$CH_3CH_2OH + 2MnO_2 + 3H^+ \rightarrow CH_3COO^- + 2Mn^{2+} + 3H_2O$	DRM3
(5,1)	$CH_3CH_2OH + 4FeOOH + 7H^+ \rightarrow CH_3COO^- + 4Fe^{2+} + 7H_2O$	DRM2
(5,2)	$CH_3CH_2OH + 4FeOOH + 7H^+ \rightarrow CH_3COO^- + 4Fe^{2+} + 7H_2O$	DRM3
(6,1)	$CH_3CH_2OH + 0.5SO_4^{2-} \rightarrow CH_3COO^- + 0.5HS^- + 0.5H^+ + H_2O$	DRM3
(6,2)	$CH_3CH_2OH + 0.5SO_4^{2-} \rightarrow CH_3COO^- + 0.5HS^- + 0.5H^+ + H_2O$	SO4RM
(7,1)	$CH_3CH_2OH + 2S^0 + H_2O \rightarrow CH_3COO^- + 2HS^- + 3H^+$	DRM3
(7,2)	$CH_3CH_2OH + 2S^0 + H_2O \rightarrow CH_3COO^- + 2HS^- + 3H^+$	S0RM
(8,1)	$CH_3CH_2OH + 0.5HCO_3^- \rightarrow CH_3COO^- + 0.5CH_4 + 0.5H^+ + 0.5H_2O$	MGM
(9,1)	$CH_3COO^- + 2O_2 \rightarrow 2HCO_3^- + H^+$	AM
(9,2)	$CH_3COO^- + 2O_2 \rightarrow 2HCO_3^- + H^+$	DM
(10,1)	$CH_3COO^- + 1.6NO_3^- + 0.6H^+ \rightarrow 2HCO_3^- + 0.8N_2 + 0.8H_2O$	DM
(11,1)	$CH_3COO^- + NO_3^- + H_2O + H^+ \rightarrow 2HCO_3^- + NH_4^+$	DRM2
(11,2)	$CH_3COO^- + NO_3^- + H_2O + H^+ \rightarrow 2HCO_3^- + NH_4^+$	DRM3
(12,1)	$CH_3COO^- + 4MnO_2 + 7H^+ \rightarrow 2HCO_3^- + 4Mn^{2+} + 4H_2O$	DRM2
(12,2)	$CH_3COO^- + 4MnO_2 + 7H^+ \rightarrow 2HCO_3^- + 4Mn^{2+} + 4H_2O$	DRM3
(13,1)	$CH_3COO^- + 8FeOOH + 15H^+ \rightarrow 2HCO_3^- + 8Fe^{2+} + 8H_2O$	DRM2
(13,2)	$CH_3COO^- + 8FeOOH + 15H^+ \rightarrow 2HCO_3^- + 8Fe^{2+} + 8H_2O$	DRM3
(14,1)	$CH_3COO^- + SO_4^{2-} \rightarrow 2HCO_3^- + HS^-$	DRM3
(14,2)	$CH_3COO^- + SO_4^{2-} \rightarrow 2HCO_3^- + HS^-$	SO4RM
(15,1)	$CH_3COO^- + 4S^0 + 4H_2O \rightarrow 2HCO_3^- + 4HS^- + 5H^+$	DRM3
(15,2)	$CH_3COO^- + 4S^0 + 4H_2O \rightarrow 2HCO_3^- + 4HS^- + 5H^+$	S0RM
(16,1)	$CH_3COO^- + H_2O \rightarrow HCO_3^- + CH_4$	MGM
(17,1)	$CH_3CH_2OH + 2UO_2(CO_3)_2^{2-} + H_2O \rightarrow CH3COO^- + 4HCO_3^- + 2UO_2(s) + H^+$	DRM2
(17,2)	$CH_3CH_2OH + 2UO_2(CO_3)_2^{2-} + H_2O \rightarrow CH3COO^- + 4HCO_3^- + 2UO_2(s) + H^+$	DRM3
(17,3)	$CH_3CH_2OH + 2UO_2(CO_3)_2^{2-} + H_2O \rightarrow CH3COO^- + 4HCO_3^- + 2UO_2(s) + H^+$	SO4RM
(17,4)	$CH_3CH_2OH + 2UO_2(CO_3)_2^{2-} + H_2O \rightarrow CH3COO^- + 4HCO_3^- + 2UO_2(s) + H^+$	S0RM
(18,1)	$CH_3COO^- + 4UO_2(CO_3)_2^{2-} + 4H_2O \rightarrow 10HCO_3^- + 4UO_2(s) + H^+$	DRM2
(18,2)	$CH_3COO^- + 4UO_2(CO_3)_2^{2-} + 4H_2O \rightarrow 10HCO_3^- + 4UO_2(s) + H^+$	DRM3
(18,3)	$CH_3COO^- + 4UO_2(CO_3)_2^{2-} + 4H_2O \rightarrow 10HCO_3^- + 4UO_2(s) + H^+$	SO4RM
(18,4)	$CH_3COO^- + 4UO_2(CO_3)_2^{2-} + 4H_2O \rightarrow 10HCO_3^- + 4UO_2(s) + H^+$	S0RM

Table 4. Secondary redox reactions (SRRs)

Number	Reaction
(1)	$0.5Mn^{2+}(aq) + 0.25O_2 + 0.5H_2O \rightarrow 0.5MnO_2 + H^+$
(2)	$0.5{\equiv}Mn^+ + 0.25O_2 + 0.25H_2O \rightarrow 0.5MnO_2 + 0.5H^+$
(3)	$0.5MnCO_3 + 0.25O_2 + 0.5H_2O \rightarrow 0.5MnO_2 + 0.5HCO_3^- + 0.5H^+$
(4)	$Fe^{2+}(aq) + 0.25O_2 + 1.5H_2O \rightarrow FeOOH + 2H^+$
(5)	${\equiv}Fe^+ + 0.25O_2 + 1.0H_2O \rightarrow FeOOH + H^+$
(6)	$FeCO_3 + 0.25O_2 + 1.5H_2O \rightarrow FeOOH + HCO_3^- + H^+$
(7)	$HS^- + 2O_2 \rightarrow SO_4^{2-} + H^+$
(8)	$S^0 + 1.5O_2 + H_2O \rightarrow SO_4^{2-} + 2H^+$
(9)	$FeS + 2O_2 \rightarrow Fe^{2+} + SO_4^{2-}$
(10)	$CH_4 + 2O_2 \rightarrow HCO_3^- + H^+ + H_2O$
(11)	$Fe^{2+}(aq) + 0.2NO_3^- + 1.4H_2O \rightarrow FeOOH + 0.1N_2 + 1.8H^+$
(12)	${\equiv}Fe^+ + 0.2NO_3^- + 1.4H_2O \rightarrow FeOOH + 0.1N_2 + 0.8H^+$
(13)	$FeCO_3 + 0.2NO_3^- + 1.4H_2O \rightarrow FeOOH + HCO_3^- + 0.1N_2 + 0.8H^+$
(14)	$HS^- + 1.6NO_3^- + 0.6H^+ \rightarrow SO_4^{2-} + 0.8N_2 + 0.8H_2O$
(15)	$S^0 + 1.2NO_3^- + 0.4H_2O \rightarrow SO_4^{2-} + 0.6N_2 + 0.8H^+$
(16)	$FeS + 1.6NO_3^- + 1.6H^+ \rightarrow Fe^{2+} + SO_4^{2-} + 0.8N_2 + 0.8H_2O$
(17)	$Fe^{2+}(aq) + 0.5MnO_2 + H_2O \rightarrow FeOOH + 0.5Mn^{2+} + H^+$
(18)	${\equiv}Fe^+ + 0.5MnO_2 + 0.5H_2O \rightarrow FeOOH + 0.5Mn^{2+} + H^+$
(19)	$FeCO_3 + 0.5MnO_2 + H_2O \rightarrow FeOOH + 0.5Mn^{2+} + HCO_3^-$
(20)	$0.5HS^- + 0.5MnO_2 + 1.5H^+ \rightarrow 0.5S^0 + 0.5Mn^{2+} + H_2O$
(21)	$FeS + 1.5MnO_2 + 3H^+ \rightarrow FeOOH + S^0 + 1.5Mn^{2+} + H_2O$
(22)	$0.5HS^- + FeOOH + 3H^+ \rightarrow 0.5S^0 + Fe^{2+} + 2H_2O$
(23)	$4S^0 + 4H_2O \rightarrow 3HS^- + SO_4^{2-} + 5H^+$
(24)	$0.125NH_4^+ + 0.25O_2 \rightarrow 0.125NO_3^- + 0.125H_2O + 0.25H^+$
(25)	$UO_2(s) + 0.5O_2 + 2HCO_3^- \rightarrow UO_2(CO_3)_2^{2-} + H_2O$
(26)	$UO_2(s) + 0.4NO_3^- + 2HCO_3^- + 0.4H^+ \rightarrow UO_2(CO_3)_2^{2-} + 0.2N_2 + 1.2H_2O$
(27)	$UO_2(s) + MnO_2 + 2HCO_3^- + 2H^+ \rightarrow UO_2(CO_3)_2^{2-} + Mn^{2+} + 2H_2O$

Table 5. Mineral precipitation reactions (MPRs)

Number	Reaction
(1)	$Mn^{2+}(aq) + CO_3^{2-} = MnCO_3$
(2)	$Fe^{2+}(aq) + CO_3^{2-} = FeCO_3$
(3)	$Fe^{2+}(aq) + HS^- = FeS + H^+$
(4)	$Fe^{2+}(ads) + HS^- = FeS$
(5)	$FeCO_3 + HS^- = FeS + HCO_3^-$

Table 6. Biosynthetic reaction pathways

Number	Reaction
(1)	$0.25HCO_3^- + 0.05NH_4^+ + 1.2H^+ + e^- \rightarrow 0.05C_5H_7O_2N + 0.65H_2O$
(2)	$0.179HCO_3^- + 0.0357NO_3^- + 1.214H^+ + e^- \rightarrow 0.0357C_5H_7O_2N + 0.571H_2O$
(3)	$0.217HCO_3^- + 0.0217N_2 + 1.217H^+ + e^- \rightarrow 0.0435C_5H_7O_2N + 0.564H_2O$

Table 7. Key end-products of equilibrium speciation reactions (see Tableau for summary of reactions)

Name	Fortran Name	Description	Role in Simulation
Mn^{2+}(aq)	Mn2aq	Conc of aqueous Mn^{2+}	Participation in SRRs, MPRs
Mn^{2+}(ads)	Mn2ads	Conc of adsorbed Mn^{2+}	Attenuation of MnO_2 reduction; participation in SRRs
Fe^{2+}(aq)	Fe2aq	Conc of aqueous Fe^{2+}	Participation in SRRs, MPRs
Fe^{2+}(ads)	Fe2ads	Conc of adsorbed Fe^{2+}	Attenuation of FeOOH reduction; participation in SRRs, MPRs
{CH_3COO^-}	aCH3COO	Activity of CH_3COO^-	Free energy of TEAPs, SRRs
{NO_3^-}	aNO3	Activity of NO_3^-	Free energy of TEAPs, SRRs
{$UO_2(CO_3)_2^{2-}$}	aUO2CO32	Activity of U(VI)-carbonate	Free energy of TEAPs, SRRs
{SO_4^{2-}}	aSO4	Activity of SO_4^{2-}	Free energy of TEAPs, SRRs
{NH_4^+}	aNH4	Activity of NH_4^+	Free energy of TEAPs, SRRs
{H^+}*	aH	Activity of H^+	Free energy of TEAPs, SRRs
{Mn^{2+}}	aMn2aq	Activity of Mn^{2+}(aq)	Free energy of TEAPs, SRRs, MPRs
{Fe^{2+}}	aFe2aq	Activity of Fe^{2+}(aq)	Free energy of TEAPs, SRRs, MPRs
{HS^-}	aHS	Activity of HS^-	Free energy of TEAPs, SRRs, MPRs
{HCO_3^-}	aHCO3	Activity of HCO_3^-	Free energy of TEAPs, SRRs, MPRs
{CH_4(aq)}	aCH4	Activity of CH_4(aq)	Free energy of TEAPs, SRRs, MPRs

TEAPs = Terminal Electron Accepting Processes
SRRs = Secondary Redox Reactions
MPRs = Mineral Precipitation Reactions

* pH was fixed at 6.9 for the simulation of the Area 2 sediment slurry experiment

Table 8. General TEAP kinetic reaction equations

Soluble electron acceptors

RTEAP(i,j) = Vmax(i,j)*FED(i,j)*FEA(i,j)*FTTEAP(i)*FIED(i,j)*FIEA(i,j)*BM(i) (mol e^- L^{-1} d^{-1})

Vmax(i,j) = μmax(i,j)/YCells(i,j)
μmax = maximum specific growth rate for cells catalyzing RTEAP(i,j) (d^{-1})
YCells(i,j) = Yield coefficient for RTEAP(i,j) (mol cells/electron)
= fs0(i,j)*gmwcells/biomasscoefdenom(i,j))

Solid-phase electron acceptors

RTEAP(i,j) = Vmax(i,j)*FED(i,j)*FEA(i,j)*FTTEAP(i)*FIED(i,j)*FIEA(i,j)*BM(i)´/(KmDRM(i)+BM(i)´)

Vmax(i,j) = VmaxEA(i,j) × EAfss **(solid-phase electron acceptors)**
VmaxEA(i,j) = maximum reduction rate constant at high biomass (mol/mol sites/d)
EAfss = concentration of free surface sites (mol L^{-1})

BM(i)´ = BM(i)/Eafss (g cells/mol free surface sites)
KmDRM(i) = half-saturation constant for the biomass-dependent rate of e^- transfer to free surface sites (g cells/mol free surface sites)

FED(i,j) = ED(i)/(KmED(i,j) + ED(i))
ED(i) = concentration of e^- donor for TEAP(i) (mol L^{-1})
KmED(i,j) = half-saturation constant for uptake of ED(i) via RTEAP(i,j) (mol L^{-1})

FEA(i,j) = EA(i)/(KmED(i,j) + EA(i))
EA(i) = concentration of e^- acceptor TEAP(i) (mol L^{-1})
KmEA(i,j) = half-saturation constant for uptake of EA(i) via RTEAP(i,j) (mol L^{-1})

FTTEAP(i) = max(0, (1-exp(dGrxnTEAP(i) × nelecTEAP(i)-dGmin(i))/0.008314/(273 + Temp))))
dGrxnTEAP(i) = free energy for TEAP(i) (kJ/electron)
nelecTEAP(i) = number of e^- transferred in TEAP(i)
dGmin(i) = minimum free energy for biological energy conservation (-20 kJ/rxn)
Temp = temperature (K)

$$FIED(i,j) = \prod_k KmIED(i,j,k)/(KmIED(i,j,k) + EDI(i,j,k))$$
KmIED(i,j,k) = half-saturation concentration of e^- donor k inhibiting RTEAP(i,j)
EDI(i,j,k) = concentration of e^- donor k inhibiting RTEAP(i,j)

$$FIEA(i,j) = \prod_k KmIEA(i,j,k)/(KmIEA(i,j,k) + EAI(i,j,k))$$
KmIEA(i,j,k) = half-saturation concentration of e^- acceptor k inhibiting RTEAP(i,j)
EAI(i,j,k) = concentration of e^- acceptor k inhibiting RTEAP(i,j)

BM(i) = Biomass of micoorganisms catalyzing TEAP(i) (g cells L^{-1})

Table 9. General TEAP reactant/product flux equations

---

1. Electron Donors

$$RED(i) = \sum_{j} RTEAP(i,j) \times Reaccoef(i,1) \text{ (mol } L^{-1}\ d^{-1})$$

Where:

RED(i) = total rate of e^- donor consumption coupled to TEAP(i) (mol e^- L^{-1} d^{-1})
RTEAP(i,j) = rate of e^- transfer coupled to RTEAP(i,j) (mol e^- L^{-1} d^{-1})
Reaccoef(i,1) = mol e^- donor consumed per e^- in TEAP(i) (mol/mol e^-)

2. Electron Acceptors

$$REA(i) = \sum_{j} fe0(i,j) \times RTEAP(i,j) \times Reaccoef(i,2) \text{ (mol } L^{-1}\ d^{-1})$$

Where:

REA(i) = total rate of e^- acceptor consumption coupled to TEAP(i) (mol e^- L^{-1} d^{-1})
fe0(i,j) = fraction of e^- donor used in RTEAP(i,j) that goes toward energy generation
Reaccoef(i,2) = mol e^- acceptor consumed per e^- transferred in TEAP(i) (mol/mol e^-)
(see below for additional definitions)

3. Other Reactants

$$ROR(i) = \sum_{j} fe0(i,j) \times RTEAP(i,j) \times Reaccoef(i,k) \text{ (mol } L^{-1}\ d^{-1})$$

Where:

ROR(i) = total rate of other reactant consumption coupled to TEAP(i) (mol L^{-1} d^{-1})
Reaccoef(i,k) = mol reactant k consumed per e^- transferred in TEAP(i) (mol/mol e^-)

4. Reaction End Products

$$REP(i) = \sum_{j} fe0(i,j) \times RTEAP(i,j) \times Prodcoef(i,k) \text{ (mol } L^{-1}\ d^{-1})$$

Where:

REP(i) = total rate of end product accumulation coupled to TEAP(i) (mol L^{-1} d^{-1})
Reaccoef(i,k) = mol end product k produced per e^- transferred in TEAP(i) (mol/mol e^-)
fe0(i,j) = 1.0 - fs0(i,j)
fs0(i,j) = 1.0/(1 + A)
A = -(dGp(i,j)/(epsiln(i,j)^ndenom(i)) + dGpC(i,j)/epsiln(i,j))/(dGrxnTEAP(i) × epsiln(i,j))
dGp(i,j) = dGfPyruvate - dGc0(i,j)
dGfPyruvate = ΔG_f of pyruvate (assumed to be the central biosynthetic intermediate in the synthesis of cellular organic carbon)

Table 9. Continued

$$dGc0(i,j) = FEDCS(i,j,k) \times dGc0EDCS(i,j,k) + \left(1 - \sum_{k} FEDCS(i,j,k)\right) \times dGc0HCO3$$

FEDCS(i,j,k)= function depicting kinetic control on utilization of organic e^- donor as a carbon source for production of BM(i) via RTEAP(i,j) *(see yield.f90 for details)*

dGc0ED(i,j,k) = free energy required to synthesize organic e^- donor k from HCO_3^-

dGcHCO3 = free energy required to liberate an electron from H_2O for use in HCO_3^- fixation

epsiln(i,j) = energy transfer efficiency for RTEAP(i,j)

dGpc(i,j) = free energy required to synthesize biomass

= FNNH4(i)*dGpCNH4+FNNO3(i)*dGpCNO3+FNN2(i)*dGpCN2

FNNH4(i) = fraction of cellular nitrogen obtained from NH_4^+

dGpCNH4 = free energy required to synthesize biomass with NH_4^+ as a N source

FNNO3(i) = fraction of cellular nitrogen obtained from NO_3^-

dGpCNO3 = free energy required to synthesize biomass with NO_3^- as a N source

FNN2(i) = fraction of cellular nitrogen obtained from N_2

dGpCN2 = free energy required to synthesize biomass with N_2 as a N source

(see below for additional definitions)

Table 10. Microbial biosynthesis and nitrogen metabolism equations

---

1. Microbial Biosynthesis

$$RBM(i) = \sum_{i^*, j^*} fs0(i, j) \times RTEAP(i^*, j^*) \times Prodcoef BS(i, j,1) \times gmwcells \ (\text{mol } L^{-1} \ d^{-1})$$

Where:

RBM(i) = Total rate of BM(i) biosynthesis (g cells L^{-1} d^{-1})
fs0(i,j) = Fraction of e^- donor used to produce biomass in RTEAP(i*,j*)
RTEAP(i*,j*) = Rate of electron transfer coupled to RTEAP(i*,j*) (mol e^- L^{-1} d^{-1})
i*, j* refer to RTEAPs that involve BM(i)
ProdcoefBS(i,j,1) = mol cells produced per e^- in biosynthesis coupled to RTEAP(i*,j*)
ProdcoefBS(i,j,1)=FNNH4(i,j)*0.05+FNNO3(i,j)*0.0357+FNN2(i,j)*0.0435
biomasscoefdenom(i,j)=FNNH4(i,j)*20.0+FNNO3(i,j)*28.0+FNN2(i,j)*23.0
(see section 2 for further definition of terms)
gmwcells = molecular weight of cell biomass (g/mol)

2. Microbial Nitrogen Metabolism

RNTot(i,j) = Total rate of N uptake for biosynthesis
= fs0(i,j) × RTEAP(i*,j*) × ReaccoefBS(i,j,2) × gmwcells
ReaccoefBS(i,j,1)=FNNH4(i,j)*0.25+FNNO3(i,j)*0.179+FNN2(i,j)*0.217
ReaccoefBS(i,j,2)=FNNH4(i,j)*0.05+FNNO3(i,j)*0.0357+FNN2(i,j)*0.0435
RNNH4(i,j) = Rate of NH_4^+ consumption for biosynthesis coupled to RTEAP(i,j)
= FNNH4(i,j)*RNTot(i,j)
RNNO3(i,j) = Rate of NO_3^- consumption for biosynthesis coupled to RTEAP(i,j)
= FNNO3(i,j)*RNTot(i,j)
RNN2(i,j) = Rate of N_2 consumption for biosynthesis coupled to RTEAP(i,j)
= FNN2(i,j)*RNTot(i,j)
FNNH4(i,j) = NH4/(KmNH4(i,j)+NH4N)
KmNH4 = half saturation constant for uptake of NH_4^+ coupled to RTEAP(i,j)
FNNO3(i,j)=(1-FNNH4(i,j))*(NO3/(KmNO3(i,j)+NO3))
KmNO3 = half saturation constant for uptake of NO_3^- coupled to RTEAP(i,j)
FNN2(i,j)=(1-FNNH4(i,j))*(1-(NO3/(KmNO3(i,j)+NO3)))
KmN2 = half saturation constant for uptake of N_2 coupled to RTEAP(i,j)

Table 11. Secondary redox reaction equations

$RSRR(i) = kRedOxid \times Red \times Oxid \times FTSRR(i,j)$

Where:

kRedOxid = second-order reaction rate coefficient $(mol\ L^{-1})^{-1}d^{-1}$
Red = Concentration of reducing reactant
Oxid = Concentration of oxidizing reactant
$FTSRR(i) = \max(0, (1-\exp(dGrxnSRR(i))/0.008314/(273 + Temp))))$
dGrxnSRR(i) = free energy for SRR(i) (kJ/electron)
Temp = temperature (K)

Table 12. Mineral recipitation equations

$RMPR(i) = kprecip(i) \times (OMEGA(i) - 1.0), OMEGA(i) \geq 1$
$RMPR(i) = kdiss(i) \times Min(i) \times (OMEGA(i) - 1.0), OMEGA(i) < 1$

Where:

$kprecip(i)$ = mineral i precipitation rate constant (mol L^{-1} d^{-1})
$kdiss(i)$ = mineral i dissoluation rate constant (d^{-1})
$Min(i)$ = concentration of mineral i (mol L^{-1})
$OMEGA(i) = \exp(dGrxnMPR(i)/0.008314/(273 + Temp))$
dGrxnMPR(i) = free energy for RMPR(i) (kJ/mol)
Temp = temperature (I)

Table 13. Parameter values used in simulation of the sediment slurry experiment. (I) Independent, (C) Constrained, (A) Arbitrary, and (M) Model-derived parameters. (NA) Not Applicable.

Description	Parameter	Value	Units	Type	Source
Maximum growth rate	umax(1,1)	5.0	d^{-1}	C	(Rittmann and McCarty, 2001)
	umax(1,2)	5.0	d^{-1}	C	(Rittmann and McCarty, 2001)
	umax(2,1)	3.0	d^{-1}	C	(Rittmann and McCarty, 2001)
	umax(3,1)	2.0	d^{-1}	C	(Rittmann and McCarty, 2001)
	umax(3,2)	2.0	d^{-1}	C	(Rittmann and McCarty, 2001)
	umax(3,3)	2.0	d^{-1}	C	(Rittmann and McCarty, 2001)
	umax(6,1)	1.5	d^{-1}	M	
	umax(6,2)	1.5	d^{-1}	M	
	umax(7,1)	1.5	d^{-1}	M	
	umax(7,2)	1.5	d^{-1}	M	
	umax(8,1)	0.5	d^{-1}	M	
	umax(9,1)	5.0	d^{-1}	C	(Rittmann and McCarty, 2001)
	umax(9,2)	5.0	d^{-1}	C	(Rittmann and McCarty, 2001)
	umax(10,1)	3.0	d^{-1}	C	(Rittmann and McCarty, 2001)
	umax(11,1)	2.0	d^{-1}	C	(Rittmann and McCarty, 2001)
	umax(11,2)	2.0	d^{-1}	C	(Rittmann and McCarty, 2001)
	umax(14,1)	2.0	d^{-1}	M	
	umax(14,2)	1.5	d^{-1}	M	
	umax(15,1)	1.5	d^{-1}	M	
	umax(15,2)	1.5	d^{-1}	M	
	umax(16,1)	0.5	d^{-1}	M	
	umax(17,1)	1.5	d^{-1}	M	
	umax(17,2)	1.5	d^{-1}	M	
	umax(17,3)	1.5	d^{-1}	M	
	umax(17,4)	1.5	d^{-1}	M	
	umax(18,1)	1.5	d^{-1}	M	
	umax(18,2)	1.5	d^{-1}	M	
	umax(18,3)	1.5	d^{-1}	M	
	umax(18,4)	1.5	d^{-1}	M	

Description	Parameter	Value	Units	Type	Source
Oxide mineral surface area	SAMnO2	170	$m^2\ g^{-1}$	A	
	SAFeOOH	170	$m^2\ g^{-1}$	C	
Maximum surface area-specific oxide mineral reduction rate	VmaxDMRM(1)	0.75	mol/mol sites/d	C/M	(Roden and Sedo, 2003)
	VmaxDMRM(2)	0.75	mol/mol sites/d	C/M	(Roden and Sedo, 2003)
	VmaxDIRM(1)	0.75	mol/mol sites/d	C/M	(Roden and Sedo, 2003)
	VmaxDIRM(2)	0.75	mol/mol sites/d	C/M	(Roden and Sedo, 2003)
Half-saturating cell density for oxide mineral reduction	KmDMRM(1)	2.25	g/mol sites	C/M	(Roden and Sedo, 2003)
	KmDMRM(2)	2.25	g/mol sites	C/M	(Roden and Sedo, 2003)
	KmDIRM(1)	2.25	g/mol sites	C/M	(Roden and Sedo, 2003)
	KmDIRM(2)	2.25	g/mol sites	C/M	(Roden and Sedo, 2003)
Cell death rate constant	kDeath(1)	0.2	d^{-1}	C	(Rittmann and McCarty, 2001)
	kDeath(2)	0.2	d^{-1}	C	(Rittmann and McCarty, 2001)
	kDeath(3)	0.05	d^{-1}	C	(Rittmann and McCarty, 2001)
	kDeath(4)	0.05	d^{-1}	C	(Rittmann and McCarty, 2001)
	kDeath(5)	0.05	d^{-1}	C	(Rittmann and McCarty, 2001)
	kDeath(6)	0.05	d^{-1}	C	(Rittmann and McCarty, 2001)
	kDeath(7)	0.05	d^{-1}	C	(Rittmann and McCarty, 2001)
	kDeath(8)	0.05	d^{-1}	C	(Rittmann and McCarty, 2001)
Decayable fraction of dead cells	fdecay	0.9		A	
Half-saturation constant for electron donor uptake	KmED(1,1)	0.000001	mol L^{-1}	A	
	·	0.000001	mol L^{-1}	A	
	·	0.000001	mol L^{-1}	A	
	·	0.000001	mol L^{-1}	A	
	KmED(18,2)	0.000001	mol L^{-1}	A	

Description	Parameter	Value	Units	Type	Source
Half-saturation constant for electron acceptor uptake	KmEA(1,1)	0.000001	mol L^{-1}	A	
	·	0.000001	mol L^{-1}	A	
	·	0.000001	mol L^{-1}	A	
	·	0.000001	mol L^{-1}	A	
	KmEA(4,2)	0.000001	mol L^{-1}	A	
	KmEA(5,1)	0.0001	mol L^{-1}	M	
	KmEA(5,2)	0.0001	mol L^{-1}	M	
	KmEA(6,1)	0.0001	mol L^{-1}	C	(Roden and Tuttle, 1993)
	KmEA(6,2)	0.0001	mol L^{-1}	C	(Roden and Tuttle, 1993)
	KmEA(7,1)	0.0001	mol L^{-1}	A	
	KmEA(7,2)	0.0001	mol L^{-1}	A	
	KmEA(8,1)	NA			
	KmEA(9,1)	0.000001	mol L^{-1}	A	
	·	0.000001	mol L^{-1}	A	
	·	0.000001	mol L^{-1}	A	
	·	0.000001	mol L^{-1}	A	
	KmEA(12,2)	0.000001	mol L^{-1}	A	
	KmEA(13,1)	0.0001	mol L^{-1}	M	
	KmEA(13,2)	0.0001	mol L^{-1}	M	
	KmEA(14,1)	0.0001	mol L^{-1}	C	(Roden and Tuttle, 1993)
	KmEA(14,2)	0.0001	mol L^{-1}	C	(Roden and Tuttle, 1993)
	KmEA(15,1)	0.0001	mol L^{-1}	A	
	KmEA(15,2)	0.0001	mol L^{-1}	A	
	KmEA(16,1)	NA			
	KmEA(17,1)	0.000001	mol L^{-1}	C	(Roden and Scheibe, 2005)
	KmEA(17,2)	0.000001	mol L^{-1}	C	(Roden and Scheibe, 2005)
	KmEA(17,3)	0.000001	mol L^{-1}	C	(Roden and Scheibe, 2005)
	KmEA(17,4)	0.000001	mol L^{-1}	C	(Roden and Scheibe, 2005)
	KmEA(18,1)	0.000001	mol L^{-1}	C	(Roden and Scheibe, 2005)
	KmEA(18,2)	0.000001	mol L^{-1}	C	(Roden and Scheibe, 2005)
	KmEA(18,3)	0.000001	mol L^{-1}	C	(Roden and Scheibe, 2005)
	KmEA(18,4)	0.000001	mol L^{-1}	C	(Roden and Scheibe, 2005)

Description	Parameter	Value	Units	Type	Source
Half-saturation constant	KmNH4(1,1)	0.000001	mol L^{-1}	A	
For uptake of NH_4^+	·	0.000001	mol L^{-1}	A	
for biosynthesis	·	0.000001	mol L^{-1}	A	
as a nitrogen source	·	0.000001	mol L^{-1}	A	
	KmNH4(18,4)	0.000001	mol L^{-1}	A	
Half-saturation constant	KmNO3(1,1,1)	0.000001	mol L^{-1}	A	
For uptake of NO_3^-	KmNO3(1,2,1)	0.000001	mol L^{-1}	A	
as a nitrogen source	·	0.000001	mol L^{-1}	A	
for biosynthesis	·	0.000001	mol L^{-1}	A	
	·	0.000001	mol L^{-1}	A	
	KmNO3(16,1,4)	0.000001	mol L^{-1}	A	
Half-saturation constant	KmIED(1,1,1)	0.000001	mol L^{-1}	A	
for inhibition of primary	KmIED(1,2,1)	0.000001	mol L^{-1}	A	
electron donor uptake by	·	0.000001	mol L^{-1}	A	
another electron donor	·	0.000001	mol L^{-1}	A	
	·	0.000001	mol L^{-1}	A	
	KmIED(8,1)	0.000001	mol L^{-1}	A	
	KmIED(9,1,1)	0.000001	mol L^{-1}	A	
	·	NA			
	·	NA			
	·	NA			
	KmIED(16,1)	NA			
	KmIED(17,1,1)	0.000001	mol L^{-1}	A	
	KmIED(17,1,2)	0.000001	mol L^{-1}	A	
	KmIED(17,1,3)	0.000001	mol L^{-1}	A	
	KmIED(17,1,4)	0.000001	mol L^{-1}	A	
	KmIED(18,1,1)	NA			
	KmIED(18,1,2)	NA			
	KmIED(18,1,3)	NA			
	KmIED(18,1,4)	NA			

Description	Parameter	Inhibiting EA	Value	Units	Type	Source
Half-saturation constant for inhibition of primary electron acceptor (EA) uptake another electron acceptor	KmIEA(1,1,1)	NA				
	KmIEA(1,2,1)	NA				
	KmIEA(2,2,1)	O_2	0.000001	mol L^{-1}	A	
	KmIEA(3,1,1)	O_2	0.000001	mol L^{-1}	A	
	KmIEA(3,2,1)	O_2	0.000001	mol L^{-1}	A	
	KmIEA(3,2,1)	O_2	0.000001	mol L^{-1}	A	
	KmIEA(4,1,1)	O_2	0.000001	mol L^{-1}	A	
	KmIEA(4,2,1)	NO_3^-	0.000001	mol L^{-1}	A	
	KmIEA(4,2,1)	O_2	0.000001	mol L^{-1}	A	
	KmIEA(4,2,2)	NO_3^-	0.000001	mol L^{-1}	A	
	KmIEA(5,1,1)	O_2	0.000001	mol L^{-1}	A	
	KmIEA(5,2,1)	NO_3^-	0.000001	mol L^{-1}	A	
	KmIEA(5,2,1)	O_2	0.000001	mol L^{-1}	A	
	KmIEA(5,2,2)	NO_3^-	0.000001	mol L^{-1}	A	
	KmIEA(6,1,1)	O_2	0.000001	mol L^{-1}	A	
	KmIEA(6,1,2)	NO_3^-	0.000001	mol L^{-1}	A	
	KmIEA(6,1,3)	MnO_2	0.001	mol L^{-1}	M	
	KmIEA(6,1,4)	FeOOH	0.001	mol L^{-1}	M	
	KmIEA(6,2,1)	O_2	0.000001	mol L^{-1}	A	
	KmIEA(6,2,2)	NO_3^-	0.000001	mol L^{-1}	A	
	KmIEA(6,2,3)	MnO_2	0.001	mol L^{-1}	M	
	KmIEA(6,2,4)	FeOOH	0.001	mol L^{-1}	M	
	KmIEA(7,1,1)	O_2	0.000001	mol L^{-1}	A	
	KmIEA(7,1,2)	NO_3^-	0.000001	mol L^{-1}	A	
	KmIEA(7,1,3)	MnO_2	0.001	mol L^{-1}	M	
	KmIEA(7,1,4)	FeOOH	0.001	mol L^{-1}	M	
	KmIEA(7,2,1)	O_2	0.000001	mol L^{-1}	A	
	KmIEA(7,2,2)	NO_3^-	0.000001	mol L^{-1}	A	
	KmIEA(8,1,1)	O_2	0.000001	mol L^{-1}	A	
	KmIEA(8,1,2)	NO_3^-	0.000001	mol L^{-1}	A	
	KmIEA(8,1,3)	MnO_2	0.005	mol L^{-1}	M	
	KmIEA(8,1,4)	FeOOH	0.005	mol L^{-1}	M	

Description	Parameter	Inhibiting EA	Value	Units	Type	Source
	KmIEA(91,1,1)	NA				
	KmIEA(9,2,1)	NA				
	KmIEA(10,2,1)	O_2	0.000001	mol L^{-1}	A	
	KmIEA(11,1,1)	O_2	0.000001	mol L^{-1}	A	
	KmIEA(11,2,1)	O_2	0.000001	mol L^{-1}	A	
	KmIEA(11,2,1)	O_2	0.000001	mol L^{-1}	A	
	KmIEA(12,1,1)	O_2	0.000001	mol L^{-1}	A	
	KmIEA(12,2,1)	NO_3^-	0.000001	mol L^{-1}	A	
	KmIEA(12,2,1)	O_2	0.000001	mol L^{-1}	A	
	KmIEA(12,2,2)	NO_3^-	0.000001	mol L^{-1}	A	
	KmIEA(13,1,1)	O_2	0.000001	mol L^{-1}	A	
	KmIEA(13,2,1)	NO_3^-	0.000001	mol L^{-1}	A	
	KmIEA(13,2,1)	O_2	0.000001	mol L^{-1}	A	
	KmIEA(13,2,2)	NO_3^-	0.000001	mol L^{-1}	A	
	KmIEA(14,1)	O_2	0.000001	mol L^{-1}	A	
	KmIEA(14,2)	NO_3^-	0.000001	mol L^{-1}	A	
	KmIEA(14,3)	MnO_2	0.001	mol L^{-1}	M	
	KmIEA(14,4)	FeOOH	0.001	mol L^{-1}	M	
	KmIEA(14,1)	O_2	0.000001	mol L^{-1}	A	
	KmIEA(14,2)	NO_3^-	0.000001	mol L^{-1}	A	
	KmIEA(14,2,3)	MnO_2	0.001	mol L^{-1}	M	
	KmIEA(14,2,4)	FeOOH	0.001	mol L^{-1}	M	
	KmIEA(15,1,1)	O_2	0.000001	mol L^{-1}	A	
	KmIEA(15,1,2)	NO_3^-	0.000001	mol L^{-1}	A	
	KmIEA(15,1,3)	MnO_2	0.001	mol L^{-1}	M	
	KmIEA(15,1,4)	FeOOH	0.001	mol L^{-1}	M	
	KmIEA(15,2,1)	O_2	0.000001	mol L^{-1}	A	
	KmIEA(15,2,2)	NO_3^-	0.000001	mol L^{-1}	A	
	KmIEA(16,1,1)	O_2	0.000001	mol L^{-1}	A	
	KmIEA(16,1,2)	NO_3^-	0.000001	mol L^{-1}	A	
	KmIEA(16,1,3)	MnO_2	0.005	mol L^{-1}	M	
	KmIEA(16,1,4)	FeOOH	0.005	mol L^{-1}	M	
	KmIEA(17,1,1)	O_2	0.000001	mol L^{-1}	A	

	KmIEA(17,1,2)	NO_3^-	0.000001	mol L^{-1}	A
	KmIEA(17,2,1)	O_2	0.000001	mol L^{-1}	A
	KmIEA(17,2,2)	NO_3^-	0.000001	mol L^{-1}	A
	KmIEA(17,3,1)	O_2	0.000001	mol L^{-1}	A
	KmIEA(17,3,2)	NO_3^-	0.000001	mol L^{-1}	A
	KmIEA(17,4,1)	O_2	0.000001	mol L^{-1}	A
	KmIEA(17,4,2)	NO_3^-	0.000001	mol L^{-1}	A
	KmIEA(18,1,2)	NO_3^-	0.000001	mol L^{-1}	A
	KmIEA(18,2,1)	O_2	0.000001	mol L^{-1}	A
	KmIEA(18,2,2)	NO_3^-	0.000001	mol L^{-1}	A
	KmIEA(18,3,1)	O_2	0.000001	mol L^{-1}	A
	KmIEA(18,3,2)	NO_3^-	0.000001	mol L^{-1}	A
	KmIEA(18,4,1)	O_2	0.000001	mol L^{-1}	A
	KmIEA(18,4,2)	NO_3^-	0.000001	mol L^{-1}	A

Description	Parameter	Value	Units	Type	Source
Energy transfer efficiency	epsiln(1,1)	0.6		C	(Rittmann and McCarty, 2001)
	epsiln(1,2)	0.6		C	(Rittmann and McCarty, 2001)
	.	0.6		C	(Rittmann and McCarty, 2001)
	.	0.6		C	(Rittmann and McCarty, 2001)
	.	0.6		C	(Rittmann and McCarty, 2001)
	epsiln(16,1)	0.6		C	(Rittmann and McCarty, 2001)
Rate constant for secondary redox reaction	kMn2aqO2	1.0D7	(mol L^{-1})$^{-1}$ yr^{-1}	C	(Hunter et al., 1998)
	kMn2adsO2	5.0D6	(mol L^{-1})$^{-1}$ yr^{-1}	C	(VanCappellen and Wang, 1996)
	kMnCO3O2	1.0D7	(mol L^{-1})$^{-1}$ yr^{-1}	A	
	kFe2aqO2	1.0D7	(mol L^{-1})$^{-1}$ yr^{-1}	C	(Hunter et al., 1998)
	kFe2adsO2	5.0D7	(mol L^{-1})$^{-1}$ yr^{-1}	C	(VanCappellen and Wang, 1996)]
	kFeCO3O2	1.0D7	(mol L^{-1})$^{-1}$ yr^{-1}	A	
	kHSO2	1.6D5	(mol L^{-1})$^{-1}$ yr^{-1}	C	(Hunter et al., 1998)
	kS0O2	6.0D4	(mol L^{-1})$^{-1}$ yr^{-1}	A	
	kFeSO2	6.0D4	(mol L^{-1})$^{-1}$ yr^{-1}	C	(Hunter et al., 1998)

Description	Parameter	Value	Units	Type	Source
	kCH4O2	1.0D7	$(mol\ L^{-1})^{-1}\ yr^{-1}$	C	(Hunter et al., 1998)
	kUO2O2	6.0D4	$(mol\ L^{-1})^{-1}\ yr^{-1}$	A	
	kFe2aqNO3	2.0D5	$(mol\ L^{-1})^{-1}\ yr^{-1}$	I	(Weber et al., 1998)
	kFe2adsNO3	2.0D5	$(mol\ L^{-1})^{-1}\ yr^{-1}$	I	(Weber et al., 1998)
	kFeCO3NO3	2.0D5	$(mol\ L^{-1})^{-1}\ yr^{-1}$	I	(Weber et al., 1998)
	kUO2NO3	6.0D4	$(mol\ L^{-1})^{-1}\ yr^{-1}$	A	
	kHSNO3	1.6D5	$(mol\ L^{-1})^{-1}\ yr^{-1}$	A	
	kS0NO3	6.0D4	$(mol\ L^{-1})^{-1}\ yr^{-1}$	A	
	kFeSNO3	6.0D4	$(mol\ L^{-1})^{-1}\ yr^{-1}$	A	
	kFe2aqMnO2	2.0D5	$(mol\ L^{-1})^{-1}\ yr^{-1}$	C	(Hunter et al., 1998)
	kFe2adsMnO2	2.0D5	$(mol\ L^{-1})^{-1}\ yr^{-1}$	C	(Hunter et al., 1998)
	kFeCO3MnO2	2.0D5	$(mol\ L^{-1})^{-1}\ yr^{-1}$	A	
	kHSMnO2	2.0D4	$(mol\ L^{-1})^{-1}\ yr^{-1}$	C	(Hunter et al., 1998)
	kFeSMnO2	2.0D4	$(mol\ L^{-1})^{-1}\ yr^{-1}$	A	
	kUO2MnO2	2.0D4	$(mol\ L^{-1})^{-1}\ yr^{-1}$	A	
	kHSFeOOH	8.0D3	$(mol\ L^{-1})^{-1}\ yr^{-1}$	C	(Hunter et al., 1998)
	kS0disp	1.0D2	yr^{-1}	C	(Berg et al., 2003)
	kNH4O2	5.0D6	$(mol\ L^{-1})^{-1}\ yr^{-1}$	C	(Hunter et al., 1998)
Rate constant for mineral precipitation or dissolution	kprecipMnCO3	1.0D-4	$mol\ L^{-1}\ yr^{-1}$	C	(Hunter et al., 1998)
	kdissMnCO3	1.0D-4	$mol\ L^{-1}\ yr^{-1}$	C	(Hunter et al., 1998)
	kprecipFeCO3	0.0	$mol\ L^{-1}\ yr^{-1}$	M	
	kdissFeCO3	0.0	$mol\ L^{-1}\ yr^{-1}$	M	
	kprecipFeS	6.0D-5	$mol\ L^{-1}\ yr^{-1}$	C	(Hunter et al., 1998)
	kdissFeS	1.0D-4	$mol\ L^{-1}\ yr^{-1}$	C	(Hunter et al., 1998)
	kHSFe2ads	1.0D4	$(mol\ L^{-1})^{-1}\ yr^{-1}$	A	
	kHSFeCO3	1.0D4	$(mol\ L^{-1})^{-1}\ yr^{-1}$	A	
Molecular weight	MWMnO2	86.9	$g\ mol^{-1}$	I	
	MWFeOOH	89.0	$g\ mol^{-1}$	I	

Description	Parameter	Value	Units	Type	Source
Mineral surface site density	SSD	3.84D-6	sites m^{-2}	C	(Davis and Kent, 1990)
Free energy of formation (non-living materials)	dGfCH3CH2OH	-181.75	kJ mol^{-1}	I	(Thauer et al., 1977)
	dGfCH3COO	-369.41	kJ mol^{-1}	I	(Thauer et al., 1977)
	dGfPyruvate	34.2	kJ mol^{-1}	I	(Thauer et al., 1977)
	dGfO2	16.32	kJ mol^{-1}	I	(Stumm and Morgan, 1996)
	dGfNO3	-111.3	kJ mol^{-1}	I	(Stumm and Morgan, 1996)
	dGfMnO2	-460.0	kJ mol^{-1}	I	(Stumm and Morgan, 1996)
	dGfFeOOH	-487.0	kJ mol^{-1}	M	
	dGfUO2CO32	-2105.4	kJ mol^{-1}	I	(Grenthe et al., 1995)
	dGfSO4	-744.6	kJ mol^{-1}	I	(Stumm and Morgan, 1996)
	dGfS0	0.0	kJ mol^{-1}	I	(Stumm and Morgan, 1996)
	dGfHCO3	-586.8	kJ mol^{-1}	I	(Stumm and Morgan, 1996)
	dGfCO3	-527.9	kJ mol^{-1}	I	(Stumm and Morgan, 1996)
	dGfN2	-18.26	kJ mol^{-1}	I	(Stumm and Morgan, 1996)
	dGfNH4	79.37	kJ mol^{-1}	I	(Stumm and Morgan, 1996)
	dGfMn2	-228.0	kJ mol^{-1}	I	(Stumm and Morgan, 1996)
	dGfFe2	-78.87	kJ mol^{-1}	I	(Stumm and Morgan, 1996)
	dGfUO2	-979.7	kJ mol^{-1}	I	(Grenthe et al., 1995)
	dGfHS	12.05	kJ mol^{-1}	I	(Stumm and Morgan, 1996)
	dGfCH4	-34.39	kJ mol^{-1}	I	(Stumm and Morgan, 1996)
	dGfH	0.0	kJ mol^{-1}	I	(Stumm and Morgan, 1996)
	dGfH2O	-237.2	kJ mol^{-1}	I	(Stumm and Morgan, 1996)
	dGfMnCO3	-816.0	kJ mol^{-1}	I	(Stumm and Morgan, 1996)
	dGfFeCO3	-666.7	kJ mol^{-1}	I	(Stumm and Morgan, 1996)
	dGfFeS	-83.71	kJ mol^{-1}	I	(Langmuir, 1997)
Free energy of formation (other; see above)	dGc0CH3CH2OH	30.4	kJ mol^{-1}	I	
	dGc0CH3COO	26.9	kJ mol^{-1}	I	
	Gc0HCO3	-82.7	kJ mol^{-1}	I	

Description	Parameter	Value	Units	Type	Source
	dGpcNH4	18.8	kJ mol^{-1}	C	(Rittmann and McCarty, 2001)
	dGpcNO3	13.5	kJ mol^{-1}	C	(Rittmann and McCarty, 2001)
	dGpcN2	16.4	kJ mol^{-1}	C	(Rittmann and McCarty, 2001)
Molecular weight of cell biomass	gmwcells	113.0	g mol^{-1}	C	(Rittmann and McCarty, 2001)